University of Stuttgart
Institute of Space Systems

Aerothermodynamics and Design for Demise (ATD^3)
Workshop 2021

Applying Ground Experiment Findings to the Simulation of Destructive Pressure Vessel Re-entry

02 December 2021

Adam S. Pagan, Georg Herdrich

Institute of Space Systems (IRS),
University of Stuttgart, Germany

Note: Update of presentation / paper given at 11th IAASS Conference 2021 titled
Key Parameters governing the Ground Risk from Re-entering Pressure Vessel Debris

Contents

- Motivation
- Review of Key Parameters
- Experimental Study
- Parametric Study
- Conclusions

Motivation

- Pressure vessels constitute almost half of all space debris objects recovered post-entry
  → Significant ground risk
- Most appear near-intact, however the degree of degradation varies.
- Composite-Overwrapped Pressure Vessels (COPV) appear to be particularly survivable.
- We will examine key parameters affecting the demisability of both metal pressure vessels and COPV through a synthesis of analytical and experimental methods informing a parametric study.

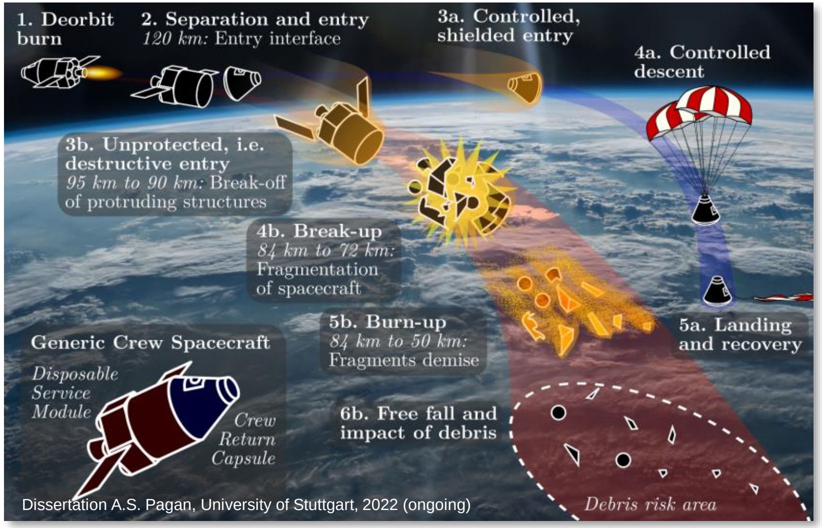

Image Source: https://www.rt.com/news/sphere-ufo-space-brazil-103/

Image Source: https://www.universetoday.com/13387/the-mysterious-case-of-two-spheres-falling-to-earth-in-australia-and-brazil/

Review of Key Parameters

Trajectory and Spacecraft Integration

- Entry trajectory of spacecraft (velocity, angle at entry interface) impact heating pulse immensely, but can hardly be optimized for demisability in practice.
- Spacecraft fragmentation (“break-up”) typically around 78 km.
- Pressure vessels are typically released in full due to connecting aluminium structures
  → Very convenient for analysis.
- Depending on integration with parent spacecraft, PV may be exposed during early entry or (partially) shielded until break-up.
- (Empty) propellant tanks typically feature low ballistic coefficient
  → Early deceleration, low heat spikes, but longer overall heating exposure

Review of Key Parameters

Aerodynamics and Geometry

- Propellant tanks are blunt objects with high “nose” radii
  → High shock stand-off distance reduces effective heat flux
- Connector residues feature low radii
  - Effects of local heating spikes very obvious on some debris items
  - Could perhaps serve as “seed points” to accelerate demise?
  - Usually only one-sided (may imply limited tumbling?)
- Tumbling motions effectively distribute heat flux over larger surface area
- Spinning motions may incur lift due to Magnus effect (varies heavily with flow regime)

Dissertation A.S. Pagan, University of Stuttgart, 2021 (ongoing)

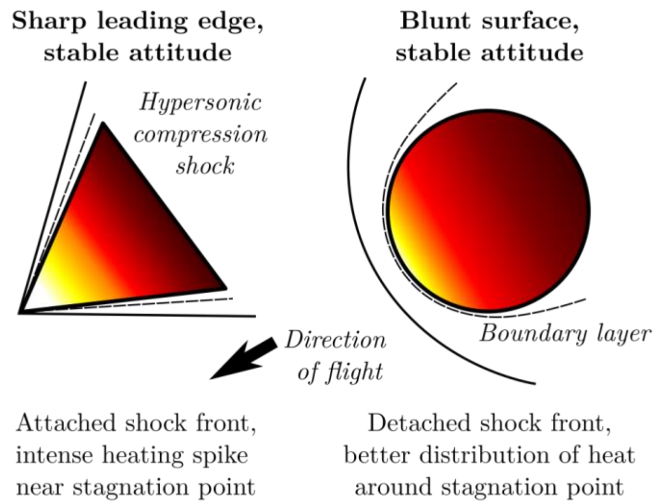

Source: https://scitechdaily.com/metal-sphere-from-orbit-hits-brazilian-town/

Source: https://boredomtherapy.com/s/brazil-metal-sphere?as=799&bdk=0

Review of Key Parameters

Thermo-Ablative Material Response

- Recovered steel and titanium PV:
  - Always oxidised, often perforated (often only one side)
  - Resolidified droplets on surface, often from protrusions or neighbouring structures (e.g. aluminium)
- Recovered COPV:
  - Usually almost intact when found
  - Overwrap slightly compromised by delamination
- Materials govern thermo-ablative response via:
  - Surface properties govern heating interface: Emissivity, catalytic properties.
  - Intrinsic thermophysical parameters govern internal heat transport: Thermal conductivity, heat capacity.
  - Phenomenology and thermodynamic implications of demise processes, e.g. melt, ablation, pyrolysis…

Image Source: AFP

Image Source: http://www.satobs.org/reentry/2008-010B/2008-010B.html

Image Source: ESA

Experimental Study

Overview

- Accumulated ESA-funded experimental activities at IRS and other institutions (see e.g. ESTIMATE database [1] and experiments at VKI, DLR, and PROMES, see e.g. [2-3]).
- **Emissivity testing:** Total and device-specific emissivities over large temperature range for pre- and post-test samples.
- **Plasma Wind Tunnel testing:** Extraction of demise-relevant properties (phenomenology effective heat of ablation, ablation threshold) in simulated entry conditions.
- **Combined:** Assessment of gas-surface interactions, specifically catalytic recombination.
- Many materials investigated. Of relevance here: aluminium alloy 7075, grade 5 titanium Ti-6Al-4V, CFRP EX1515/M55J, COPV segments.

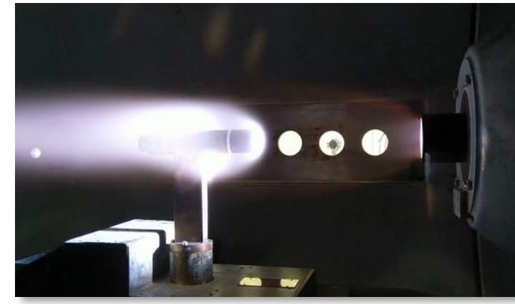

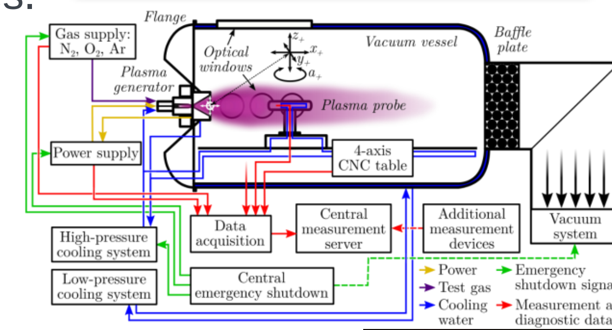

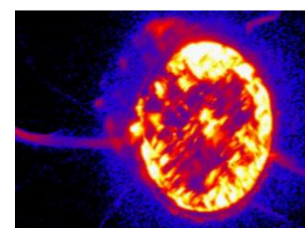

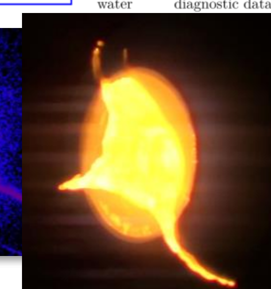

Experimental Study

Results and Observations (of Relevance here)

- **Aluminium Alloy AA7075 (and others):**
  - Oxide layer forms which can delay spillage of molten bulk
  - Time to spillage appears to scale with heat flux
  - Oxidation increases emissivity (hardly matters here)
- **Titanium Ti6Al4V:**
  - High melting temperature requires heat fluxes > 1 MW/m²
  - Emissivity dramatically increased through oxidation
  - Appears to form liquid V_2O_5 film at moderate ATD loads, generally diverse phenomenology → representativeness of separate emissivity measurements doubtful
- **CFRP & COPV segments:**
  - CFRP behaves like ablator (pyrolytic outgassing, insulation)
  - Varyingly increased propensity to delaminate
  - Mass loss rate scales roughly with heat flux

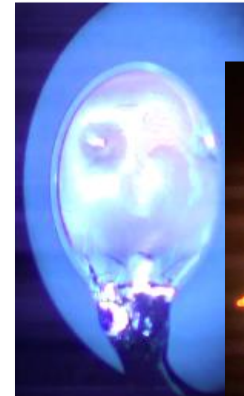

AA7075

Ti6Al4V

CFRP EX-1515/M55J

COPV segment

Parametric Study

Hollow Sphere Entry Simulation

- Simple propagator for (semi-)ballistic entries, verified via MIRKA spherical entry capsule flight data [5,6].
- PV modelled as hollow sphere with fixed physical properties (m = 8 kg, d = 600 mm, $V \approx$ 110 L). C_D varies over alt. / *Ma*.
- Three scenarios (see table), three materials evaluated: AA7075, Ti6Al4V, CFRP EX-1515/M55J → COPV
- Discretization of sphere into equiangular segments:
  - Surface heating profile scaled from stagn. pt. heat flux according to [7]
  - Local fast-tumble-averaged heating (via precession angle δ)

Scenario	Early release	Typical	Spinning
Release altitude / km	120	78	78
Flight path angle / °	-0.5	-0.835	-0.835
Velocity in air / m/s	7700	7578.5	7578.5
Precession angle / rad	0	π/6	π/2
Lift-to-drag ratio	0	0	0.3

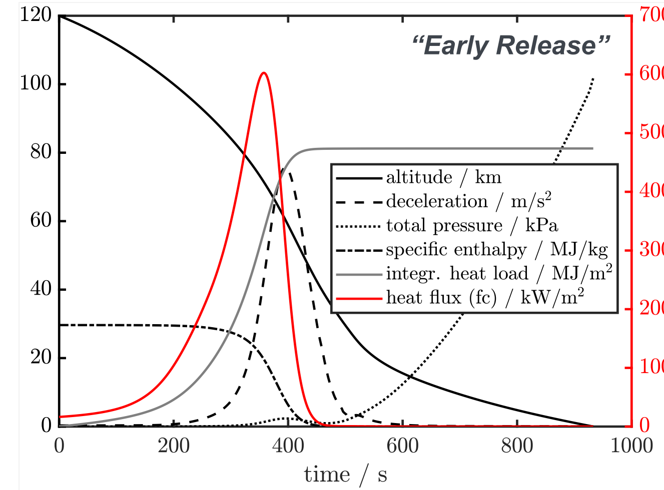

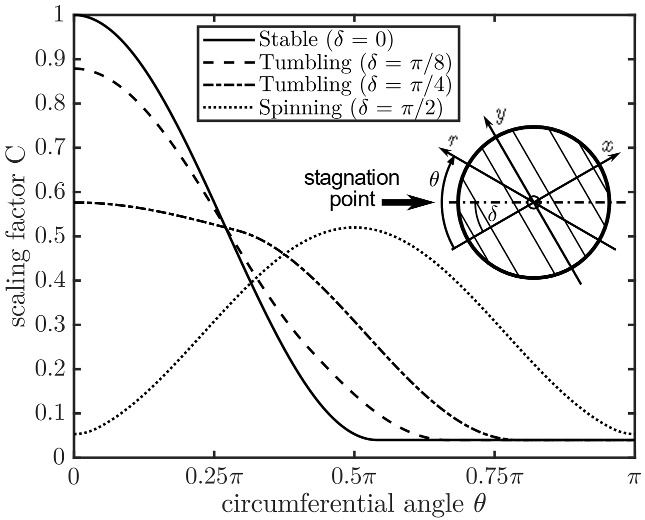

Parametric Study

Material Response Modelling

- Two criteria for perforation (local) / demise (overall):
  - **Threshold:** Critical temperature of material surpassed? $$T_{\mathrm{w,eq}} = \left(\frac{\dot{q}_{\mathrm{eff}}}{\varepsilon\sigma}\right)^{\frac{1}{4}} > T_{\mathrm{crit}}$$
  - **Calorimetric:** Sufficient heat absorbed for demise? $$\frac{Q_{\mathrm{eff}}}{H_{\mathrm{dem}}} = \frac{A_{\mathrm{segment}} \int \dot{q}_{\mathrm{eff}}\, dt}{m_0\, h_{\mathrm{abl}}} > 1$$
- Definition of h_{abl} (specifically: referenced "modular" definition of $\dot{q}_{\mathrm{eff}}$) varies depending on power of simulation tool and available input data, with $$\dot{q}_{\mathrm{eff}} = \chi_{\mathrm{cat}}\dot{q}_{\mathrm{fc}} - \varepsilon\sigma T_{\mathrm{w}}^4 - \dot{q}_{\mathrm{struct}}$$
- h_{abl} (any variant) empirically extracted from demise experiments in PWT at IRS
- T_{crit} from literature (to be refined from experiments)

Material sample / PV wall segment as a thermo-ablative "black box" represented through h_{abl}

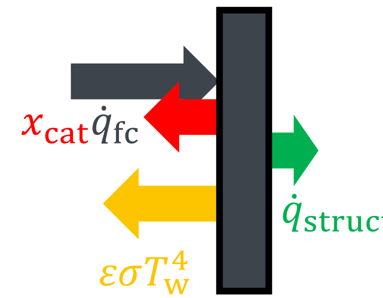

Model material properties	CFRP EX-1515/M55J	Ti6Al4V	AA7075
Density / kg/m³	1630	4421	2813
Corresponding wall thickness / mm *(constant mass)*	4.34	1.60	2.51
Critical temperature / K	500 (pyrol.) 1100 (oxid.)	1900	900
Effective heat of ablation / MJ/kg ($\dot{q}_{\mathrm{eff}} := \chi_{\mathrm{cat}}\dot{q}_{\mathrm{fc}}$)	98 (pyrol.) 45 (oxid.)	2.1	0.73

Parametric Study

Emissivity and Catalysis

- Immediate thermal equilibration assumed.
- Emissivities from EMF tests and literature [4,8].
- Baseline catalysis model from Goulard and Scott [9,10], with flight and ground test frozen BL properties approximated via NASA CEA [11].
- Non-equilibrium effects to be accounted for according to [12]. For now: Simplistic similitude correction function based on results in reference.
- Relational scaling of γ_O and γ_N from experimental data based on SiC catalysis reference from [13].

Recombination coefficients	CFRP EX-1515/M55J	Ti6Al4V	AA7075
γ_O	1	0.1393	0.0271
γ_N	1	0.1895	0.0699

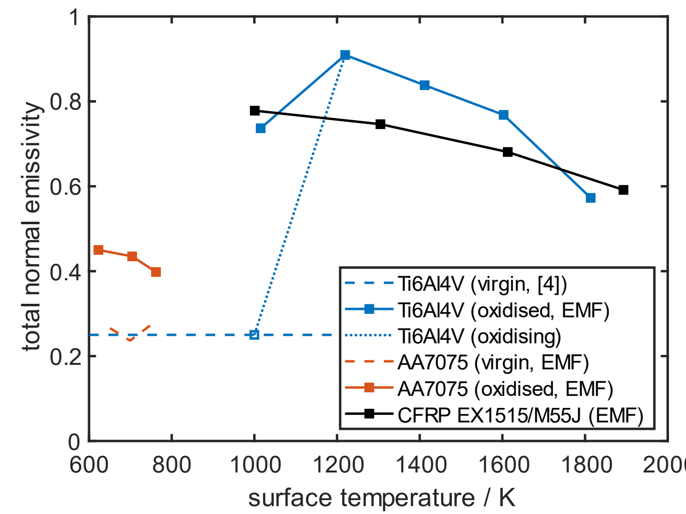

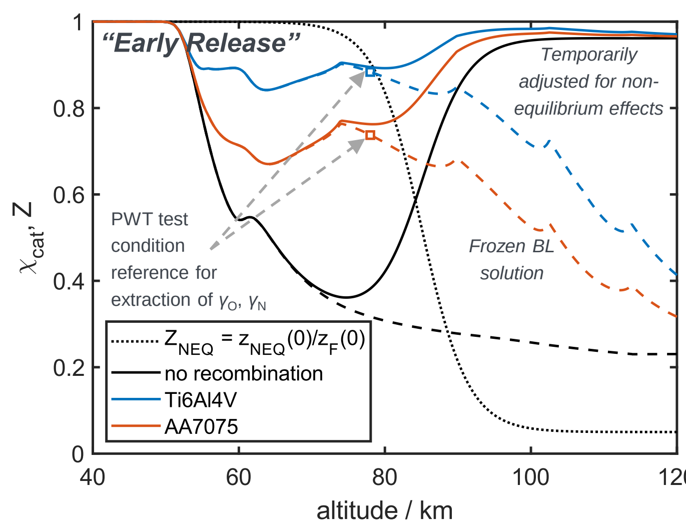

Parametric Study

Notes on Consideration of Equilibrium Effects

- Proper implementation of catalysis modelling with non-equilibrium effects ongoing (closed form analytical approximation as proposed by Inger [12])
  → update to be submitted for publication soon!
- Still working on the implementation (minor bugfixes, adaptive emissivity, etc.), but almost done!
- Example: Applied to trajectory of spherical MIRKA entry capsule (emissivity = 0.85):

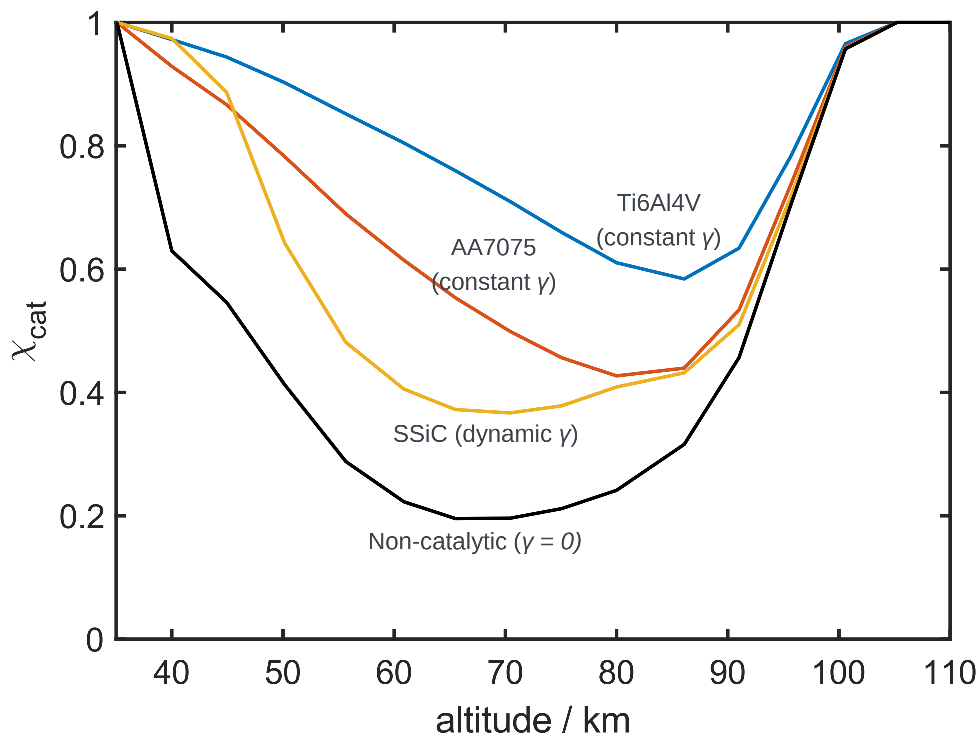

Parametric Study

Results

Material	CFRP EX-1515/M55J → COPV			Grade 5 Titanium Ti6Al4V			Aluminium Alloy AA7075		
Scenario:	*Early release*	*Typical*	*Spinning*	*Early release*	*Typical*	*Spinning*	*Early release*	*Typical*	*Spinning*
$T_{w,max}$ / K	1946	1836	1606	1811	1731	1522	1997	1931	1738
$\Delta t(T_{w,peak}>T_{crit})$ / s	464	159	427	0	0	0	406	137	366
$\left.\frac{Q_{\mathrm{eff}}}{H_{\mathrm{dem}}}\right\|_{\mathrm{global}}$	2.9%	4.2%	6.3%	124%	79.6%	116%	318%	193%	281%
$\left.\frac{Q_{\mathrm{eff}}}{H_{\mathrm{dem}}}\right\|_{\mathrm{peak}}$	9.4%	10.8%	11.4%	399%	206%	211%	1021%	500%	510%
Dominating criterion:	calorim.	calorim.	calorim.	threshold	threshold	threshold	n/a	n/a	n/a
m_{impact} / kg	7.83 (97.9%)	7.71 (96.4%)	7.34 (91.8%)	8 (100%)	8 (100%)	8 (100%)	0	0	0
$E_{kin,term}$ / J	3856	3803	3440	3939	3944	3749	0	0	0
Verdict	**CFRP overwrap is essentially an ablative TPS.** → Get rid of it, e.g. by promoting delamination?			Borderline case, threshold rarely exceeded, predicts occasional observation of punctures in recovered PV. → **Titanium is poor choice.**			**Demises reliably!**		

Summary

- Review of key parameters (trajectory, aerodynamics, geometry, materials) impacting PV demisability.
- Nature of spherical PVs provide ideal basis to extrapolate from experimental material demise research to material demise models.
- Combined testing methodology provides full picture for material-focused demise modelling (emissivity, catalysis correction, heat of ablation), catering to different model requirements
- Update coming shortly with proper consideration of full non-equilibrium effects on catalysis as proposed by Inger [12] – unfortunately not quite ready by today.
- Results match observations of recovered pressure vessel residue
- Effects of different entry trajectories and attitude states play out differently depending on material's dominance of demise criteria (threshold vs. heat).

University of Stuttgart
Institute of Space Systems

Thank you!

Dipl.-Ing. Adam S. Pagan

e-mail pagan@irs.uni-stuttgart.de
phone +49 (0) 711 685-62135
www. irs.uni-stuttgart.de

University of Stuttgart
Institute of Space Systems, Faculty 6
Pfaffenwaldring 29, 70569 Stuttgart

Literature

[1] European Space Agency. ESTIMATE: European Space maTerIal deMisability dATabasE. Ed. by L. J. Ferrer. Aug. 6, 2020. url: https://estimate.sdo.esoc.esa.int/ (visited on 27/09/2021).

[2] A. Fagnani, O. Chazot, A. Hubin, & B. Helber (2019, March). Comprehensive characterization of the aerothermomechanical response of space debris to atmospheric entry plasmas. In 10th VKI PhD Symposium.

[3] J. C. Beck, T. Schleutker and A. Guelhan, “Improved Representation of Destructive Spacecraft Re-entry from Analysis of High Enthalpy Wind Tunnel Tests of Spacecraft and Equipment,” in 69th International Astronautical Congress (IAC), Bremen, Germany, 2018.

[4] M. Balat-Pichelin, J. Annaloro, L. Barka, J.L. Sans "Behavior of TA6V Alloy at High Temperature in Air Plasma Conditions: Part 2—Thermal Diffusivity and Emissivity." Journal of Materials Engineering and Performance 29.7 (2020): 4606-4616.

[5] R. Müller-Eigner, G. Koppenwallner, and B. Fritsche. „Pressure & Heat Flux Measurement with RAFLEX II during MIRKA Re-Entry“. In: Proceedings of the 3rd European Symposium on Aerothermodynamics for Space Vehicles. Noordwijk, The Netherlands, 1998.

[6] U. Schöttle, E. Messerschmid, G. Jahn, J. Burkhardt, M. Fertig, and U. Schöttle. MIRKA - Hitzeschildexperiment: Endbericht. Tech. rep. IRS-98-P2. Institute of Space Systems, University of Stuttgart, Apr. 1998 (in German).

[7] V. K. Dogra, R. G. Wilmoth, and J. N. Moss. „Aerothermodynamics of a 1.6-meter-diameter sphere in hypersonic rarefied flow“. In: AIAA journal 30.7 (1992), pp. 1789–1794.

[8] A. S. Pagan, B. Massuti-Ballester & G. Herdrich (2016). Total and spectral emissivities of demising aerospace materials. Frontier of Applied Plasma Technology, 9(1), 7-13.

[9] R. Goulard. „On catalytic recombination rates in hypersonic stagnation heat transfer“. In: Journal of Jet Propulsion 28.11 (1958). DOI: 10.2514/8.744, pp. 737–745.

[10] C Scott. „Catalytic recombination of nitrogen and oxygen on high-temperature reusable surface insulation“. In: 15th Thermophysics Conference. 1981, p. 1477.

[11] S. Gordon and B. J. McBride, "Computer Program for Calculation of Complex Chemical Equilibrium Compositions and Applications," NASA Reference Publication 1311 (1996).

[12] G. R. Inger. R. L. Baker (2005). Nonequilibrium Viscous Shock-Layer Heat Transfer with Arbitrary Surface Catalycity”. Journal of Spacecraft and Rockets 42(2), 193-200.

[13] B. Massuti Ballester. Aerothermochemistry of High-Temperature Materials for Atmospheric Entry. (Dissertation) University of Stuttgart (2019).

Further Reading

Destructive Entry and PV demise:

- Y. Prévereaud, J.-L. Vérant, M. Balat-Pichelin, and J.-M. Moschetta. „Numerical and experimental study of the thermal degradation process during the atmospheric re-entry of a TiAl6V4 tank“. In: Acta Astronautica 122 (May 2016), pp. 258–286. doi: 10.1016/j.actaastro.2016.02.009.
- B. Fritsche, T. Lips, and G. Koppenwallner. „Analytical and Numerical Re-entry Analysis of Simple shaped Objects“. In: Acta Astronautica 60.8-9 (Apr. 2007), pp. 737–751. doi: 10.1016/j.actaastro.2006.07.017.
- T. Lips, B. Fritsche, R. Kanzler, T. Schleutker, A. Gülhan, B. Bonvoisin, T. Soares, and G. Sinnema. „About the demisability of propellant tanks during atmospheric re-entry from LEO“. In: Journal of Space Safety Engineering 4.2 (June 2017), pp. 99–104. doi: 10.1016/j.jsse.2017.07.004.
- W. Ailor, W. Hallman, G. Steckel and M. Weaver, “Analysis of Reentered Debris and Implications for Survivability Modelling,” in Proceedings of the Fourth European Conference on Space Debris, Darmstadt, Germany, 2005.
- C. Durin, “Study of Spacecraft Elements Surviving an Atmospheric Re-entry,” in Sixth IAASS Conference, Montréal, Canada, 2013.
- B. Bastida Virgili, S. Lemmens, J. Siminski und Q. Funke, „Practicalities of Re-entry Predictions - The VEGA-01 AVUM case,“ in 7th European Conference on Space Debris, 2017.
- A. S. Pagan, B. Massuti-Ballester, G. Herdrich, J. A. Merrifield, J. C. Beck, V. Liedtke and B. Bonvoisin, “Review and Analysis of Experimental Activities on the Demisability of Pressure Vessels,” in 4th Space Debris Re-entry Workshop, 2018.
- ESA-ESOC. ESA’s re-entry predictions. English. May 2021. url: https://reentry.esoc.esa.int/home/recovereddebris.

Experimental material characterisation

- A. S. Pagan, B. Massuti-Ballester, and G. Herdrich. „Total and Spectral Emissivities of Demising Aerospace Materials“. In: Frontier of Applied Plasma Technology 8(1), pp. 7–12, 2016.
- A. S. Pagan, B. Massuti-Ballester, G. Herdrich, J. Merrifield, J. Beck, V. Liedtke, and B. Bonvoisin. „Experimental Investigation of Material Demisability in Uncontrolled Earth Re-entries“. In: 31st International Symposium on Space Technology and Science. Matsuyama, Japan, 2017
- J. Merrifield, “Characterisation of Demisable Materials: Database Design and Final Report,” 2018.

Plasma Wind Tunnel method

- G. Herdrich, M. Fertig und S. Löhle, „Experimental Simulation of High Enthalpy Planetary Entries,“ The Open Plasma Physics Journal, Bd. 2, p. 150–164, 12 2009.
- S. Löhle, S. Fasoulas, G. H. Herdrich, T. A. Hermann, B. Massuti-Ballester, A. Meindl, A. S. Pagan und F. Zander, „The Plasma Wind Tunnels at the Institute of Space Systems: Current Status and Challenges,“ in 32nd AIAA Aerodynamic Measurement Technology and Ground Testing Conference, 2016.

Appendix

Trajectory Plots and Catalysis Correction for “Typical” and “Spinning” Scenarios

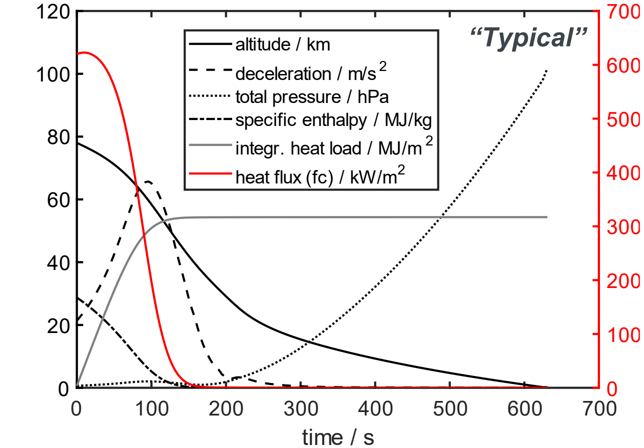

Note: LD ratio constant here. In reality, Magnus effect magnitude and sign varies considerably in different flow regimes! [9]

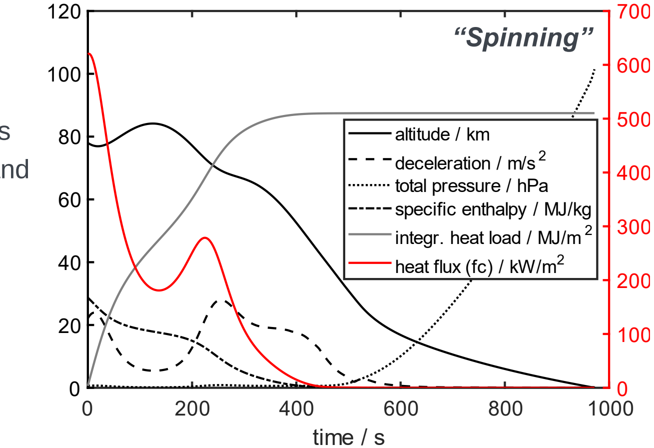

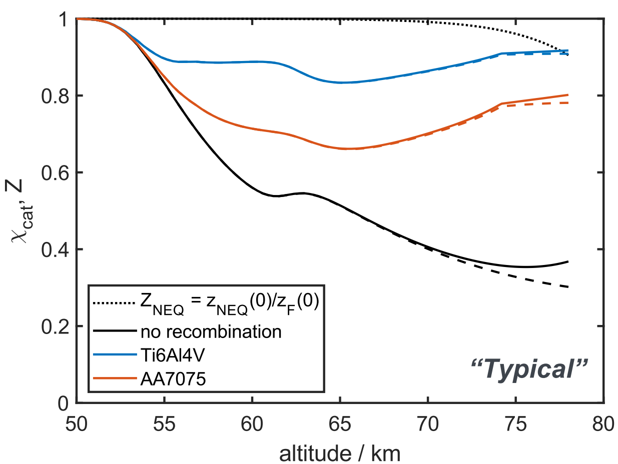

Dashed lines: Frozen BL solution

Full lines: Adjusted for non-equilibrium effects (temporary similitude function, to be replaced)